

Stabilization of the chiral phase of the $SU(6m)$ Heisenberg model on the honeycomb lattice with m particles per site for m larger than 1

Jérôme Dufour and Frédéric Mila

Institute of Physics, École Polytechnique Fédérale de Lausanne (EPFL), CH-1015 Lausanne, Switzerland

(Dated: March 5, 2024)

We show that, when N is a multiple of 6 ($N = 6m$, m integer), the $SU(N)$ Heisenberg model on the honeycomb lattice with m particles per site has a clear tendency toward chiral order as soon as $m \geq 2$. This conclusion has been reached by a systematic variational Monte Carlo investigation of Gutzwiller projected wave-functions as a function of m between the case of one particle per site ($m = 1$), for which the ground state has recently been shown to be in a plaquette singlet state, and the $m \rightarrow \infty$ limit, where a mean-field approach has established that the ground state has chiral order. This demonstrates that the chiral phase can indeed be stabilized for not too large values of m , opening the way to its experimental realisations in other lattices.

I. INTRODUCTION

Progress in cold atoms experiments has opened the door to new and exciting physics^{1–7}. When fermionic ultracold alkaline-earth atoms with nuclear spin I are trapped in optical lattices, the physics is governed by a generalized Hubbard model with $N = 2I + 1$ colors (or flavors) of fermionic particles^{8–11}. In the limit of strong on-site repulsion, when the optical wells are deep, and if the number of atoms per site is an integer, this system is in a Mott insulating phase and the low energy physics is effectively described by the $SU(N)$ Heisenberg model:

$$\hat{H} = \sum_{\langle i,j \rangle} \sum_{\alpha\beta} \hat{S}_i^{\alpha\beta} \hat{S}_j^{\beta\alpha}. \quad (1)$$

This Hamiltonian is known to exhibit various ground states depending not only on the lattice but also on the number of colors N and on the on-site $SU(N)$ symmetry of the wave function, *i.e.* the irreducible representation (irrep) labelled by a Young tableau with m boxes. For ultra-cold fermions, the case of m atoms per well corresponds to the fully antisymmetric irrep with a Young tableau consisting of a single column with m boxes. A non exhaustive list of exotic ground states contains N -flavor liquids with algebraic correlations^{12–16}, different Néel-type states with long range order^{17–19}, translational symmetry breaking states like generalized valence-bond solids^{20–26} or d -merisation ($d = 2, 3$) on a chain²⁷ and chiral spin liquids^{16,22,23,25,28–30}.

The possibility to stabilize chiral phases is particularly interesting since the search for experimental realisations in lattice models is still on-going. However, for the simple $SU(N)$ model with only nearest-neighbor Heisenberg interactions on the square lattice, unambiguous evidence of chiral order has only been obtained in the limit where N and m tend to infinity keeping the ratio $k \equiv N/m$ fixed when $k > 4$ ²². For $m = 1$, other types of order can be stabilized. For instance, exact diagonalisation results suggest that color order might be stabilized for $SU(5)$, while spontaneous dimerisation seems to take place for $SU(8)$. These results clearly call for additional investigations of the properties of the model as a function of m

for fixed k .

In this paper, our aim is to address this issue in the context of the $SU(N)$ Heisenberg models on the honeycomb lattice. This model has been studied by Szirmai *et al.*²⁹, Sinkovicz *et al.*³¹ for $k = 6$ in the mean-field limit where N and m tend to infinity keeping the ratio k fixed. They found a chiral ground state with $2\pi/3$ flux per hexagonal plaquette, and two plaquette states with higher energies: the $0\pi\pi$ plaquette in which each 0 flux plaquette is surrounded by π flux plaquettes, and a 000 plaquette phase in which hexagons are completely decoupled. However, a recent work³² done on the same lattice for $SU(6)$ in the fundamental irrep has given strong evidence in favor of the $0\pi\pi$ plaquette ground state over the chiral one with $2\pi/3$ flux. This irrep corresponds to a physical model with $m = 1$ particle per site for which Eq.1 reduces to a simple permutation Hamiltonian: $\hat{H}_{\hat{P}} = \sum_{\langle i,j \rangle} \hat{P}_{ij}$, where the constant has been omitted. It was also shown in Ref.[32] that the chiral phase can be stabilized by adding a ring-exchange term $\hat{H}_{\square} = i \sum_{\square} (\hat{P}_{\square} - \hat{P}_{\square}^{-1})$ to the Hamiltonian. Note that plaquette and chiral states can easily be distinguished experimentally by their very different signatures in the spin structure factor, as discussed in Refs.[29] and [31].

Here we explore another path to the possible stabilisation of a chiral phase for the $SU(N)$ Heisenberg model. Instead of adding a ring-exchange term, we increase the number of particles per site m for $k = 6$, and we study fully antisymmetric irreps on each site labelled by a Young tableau with m boxes in one column:

$$\square \text{ SU}(6) \quad \begin{array}{|c|} \hline \square \\ \hline \square \\ \hline \end{array} \text{ SU}(12) \quad \begin{array}{|c|} \hline \square \\ \hline \square \\ \hline \square \\ \hline \end{array} \text{ SU}(18) \dots$$

For this family of irreps, the fermionic operators \hat{c}^\dagger, \hat{c} together with the identity:

$$\hat{S}^{\alpha\beta} = \hat{c}_\alpha^\dagger \hat{c}_\beta - \frac{m}{N} \delta_{\alpha\beta} \quad (2)$$

allow the rewriting of Eq.1 as:

$$\hat{H} = \sum_{\langle i,j \rangle} \sum_{\alpha\beta} \hat{c}_{i\alpha}^\dagger \hat{c}_{i\beta} \hat{c}_{j\beta}^\dagger \hat{c}_{j\alpha} \quad (3)$$

where the constant $-zm^2/2N$ has been dropped. In the following, our goal is to investigate how the system evolves between the chiral ground state of Ref.[29] for $m = \infty$ and the $0\pi\pi$ plaquette ground state of Ref.[32] obtained for $m = 1$. We will present numerical results that give strong indication that the chiral phase is stabilized for $m > 1$.

II. VMC RESULTS

A. Method

Since our aim is to systematically study the fully anti-symmetric irreps of the $SU(6m)$ Heisenberg model on the honeycomb lattice, we need a numerical method that works for any m . Quantum Monte Carlo suffers from the sign problem, ED does not give access to large enough clusters when $m > 1$, and iPEPS has so far only given results for $m = 1$. The variational Monte Carlo (VMC) method^{33,34} is therefore the only reliable numerical method that was proven to be efficient to study more complicated representations³⁵ like the fully anti-symmetric irreps²⁷. It is not limited by the system size and recovers the mean-field results when N and m are large.

To have meaningful results we need to define a representative set of variational wave functions. Following other papers^{26,32} and inspired by the mean-field results²⁹, we have tested five different variational wave functions represented in FIG. 1, one chiral and four plaquette states. The chiral wave function is the only one having no variational parameter. It has uniform hopping amplitudes but non-uniform phase factors that creates a homogeneous flux of $2\pi/3$ per hexagonal plaquette. This wave function does not break the lattice symmetry but breaks the time reversal one. We want the other wave functions to preserve the time reversal symmetry, therefore the only allowed fluxes are 0 and π . To preserve the rotation symmetry, and since we chose unit cells containing at most 12 sites, there are only 4 non-equivalent flux configurations. Two of them have already been introduced, $0\pi\pi$ and 000 , while the other two are: $\pi 00$ consisting of a central hexagon with π flux surrounded by 0 fluxes and $\pi\pi\pi$ having a homogeneous π flux in each hexagon. Due to the simplicity of the chosen flux configurations, there are only two meaningful variational parameters, t_h and t_d : the hopping terms around the central hexagons t_h , and the hopping terms linking these hexagons t_d . Using additional hopping terms would break other symmetries, for instance having different hopping terms around the central hexagon would break the rotational symmetry. Since the honeycomb lattice is bipartite, only the relative sign of t_d and t_h matters, therefore, for the plaquette wave functions, we have a single variational free parameter, the ratio t_d/t_h with fixed $t_h = -1$.

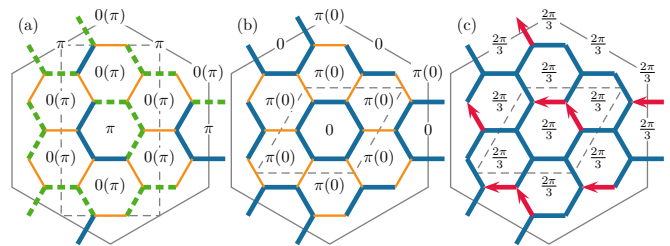


FIG. 1. Representation of the five wave functions with their unit cell on a 24-site cluster with periodic boundary conditions. (a)-(b) Plaquette wave functions, where solid blue and dashed green bonds stand for t_h and $-t_h$ respectively, while the thin yellow ones stand for t_d . By changing the sign of the ratio t_d/t_h from negative to positive, the flux configuration of the wave function will change from $\pi 00$ to $\pi\pi\pi$ in (a) and from $0\pi\pi$ to 000 in (b). (c) Chiral wave function for which the hopping terms are given by $t_{ij} = t_h e^{i2\pi/3} = t_{ji}^*$ between the sites i and j connected by a red arrow and by t_h otherwise. The flux per plaquette is defined mod 2π .

B. Results

In this section, results on a 72-site cluster with anti-periodic boundary conditions will first be presented. Then a finite size analysis on a representative example, $m = 3$, will show how accurately the thermodynamic energies can be extracted. This accuracy allows us to draw conclusions on how the VMC recovers the mean-field limit and gives new indications of a chiral phase for $m > 1$.

FIG. 2 shows the variational energies as a function of m for different values of the ratio t_d/t_h for all different wave functions on a 72-site cluster with anti-periodic boundary condition. This particular choice of boundary conditions allows us to measure the energy for $t_d/t_h = -1$ because it lifts the well-known degeneracy at the Fermi level, an important requirement to construct Gutzwiller projected wave functions. However, it does not lift the degeneracy for the value $t_d/t_h = 1$. The other missing energy is for $t_d/t_h = 0$ because the VMC fails to find a well defined starting configuration, since all hexagons are disconnected. On the lowest plot, the chiral energies are also shown as straight lines.

We can see that each plaquette wave function has at least one local minimum. While the exact position of the minima does not really matter, it is interesting to note that for all wave functions but the 000 one, the minima stay roughly stable. Indeed, we know that the 000 mean-field solution consists of disconnected hexagons with 0 flux. This solution is expected to be captured by the 000 variational wave function, when m is going to infinity for a small value of t_d/t_h . This is indeed what can be observed in the lower plot of FIG. 2: the position of the 000 minimum moves to the left when m increases but the value of its energy remains higher than the energy of both the $0\pi\pi$ and the chiral wave function. By looking more carefully at the energies of the chiral and $0\pi\pi$ wave

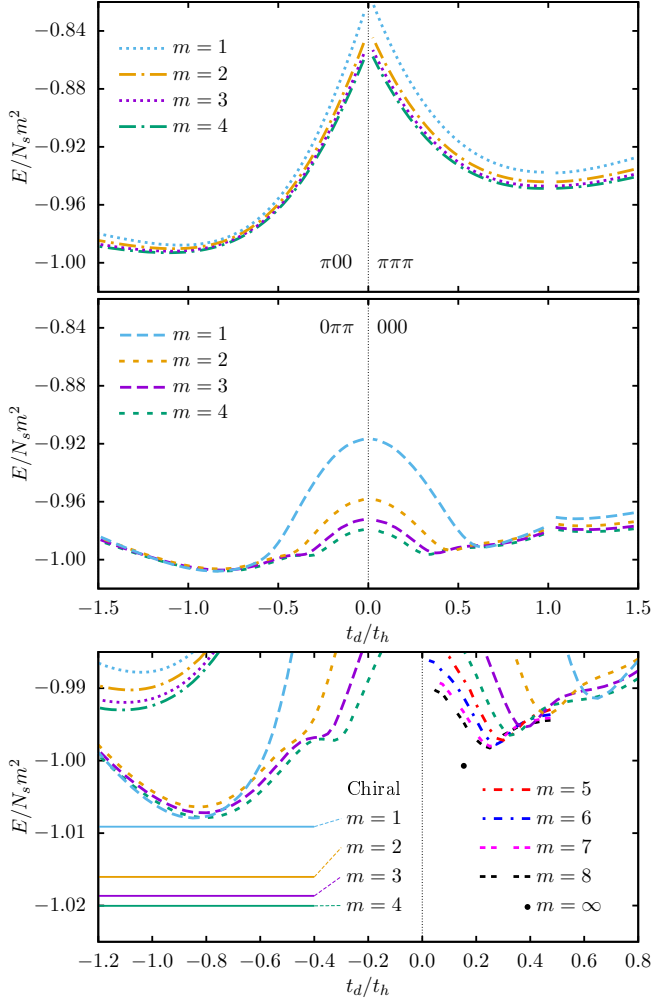


FIG. 2. Energy per site for a cluster of 72 sites. The upper and middle plots are given on the same scale to allow better comparison while the lower plot is a zoom around the minima. The error bars are smaller than the thickness of the lines. Upper plot: Energy for different values of m of the $\pi 00$ and $\pi \pi \pi$ wave functions on the left and on the right respectively. Middle plot: Energy for different values of m of the $0 \pi \pi$ and 000 wave functions on the left and on the right respectively. Lower plot: Energy of all the wave functions discussed in this paper. The energies of the chiral wave functions are represented with straight lines. Additional values for the 000 wave function for $5 \leq m \leq 8$ have been included. The filled circle corresponds to the minimal energy for the 000 wave function obtained by extrapolation in the limit $m \rightarrow \infty$. For larger systems, the extrapolated value of t_d/t_h for the 000 wave function tends to zero, as it should since the mean-field result corresponds to isolated plaquettes.

functions, it seems that the former becomes lower when m increases and the latter remains stable. This behavior is the most interesting feature of this analysis on a 72-site cluster. Indeed, there is a strong competition between the chiral and $0 \pi \pi$ wave functions when $m = 1$ and for $m > 1$ the energy of the chiral wave function becomes clearly lower.

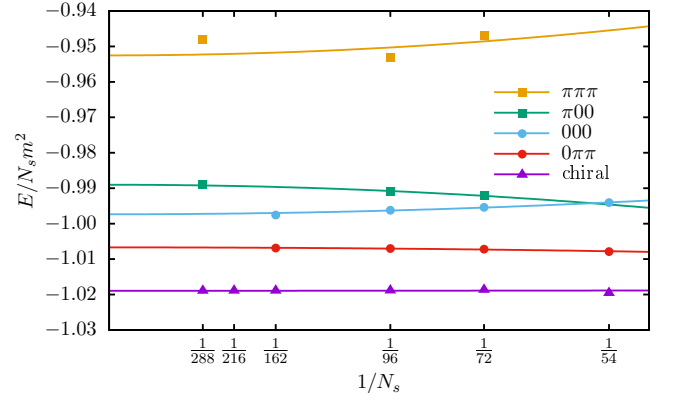


FIG. 3. Finite size scaling for $m = 3$. The function used for the fit is of the type $f(x) = ax^2 + b$ for all data sets. For some system sizes, some values are missing. This is due to a degeneracy at the Fermi level. The error bars on the points are smaller than the symbols.

The same study has been done for larger clusters (up to 288 sites) and the energies in the thermodynamic limit have been extrapolated. As an example, FIG. 3 shows the variational energies as a function of the system size for $m = 3$. It is clear that the chiral wave function gives lower energies than any of the plaquette ones no matter what the size of the system is.

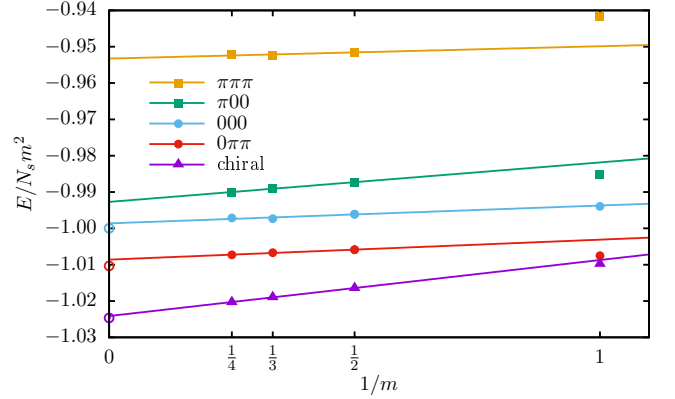


FIG. 4. Energies per site obtained by VMC in the thermodynamic limit for different irreps. They are fitted by a line based on $m = 2, 3, 4$ to show the agreement with the empty circles which are the mean-field results²⁹ valid for $m \rightarrow \infty$.

The results shown in FIG. 4 are the energies extrapolated in the thermodynamic limit. Let us first focus on already published results for the case with $m = 1$. The chiral and $0 \pi \pi$ wave function are in strong competition as already visible in FIG. 2. It was numerically concluded on the basis of extensive ED, VMC and iPEPS calculations³² that the ground state is the $0 \pi \pi$ plaquette state. In the context of our calculation, where we only calculate the energy of a single wave function, the chiral state turns out to have a slightly lower energy, but as shown in Ref.[32], if several variational wave-functions with differ-

ent boundary conditions are coupled, this small energy difference is reverted in favour of the plaquette phase.

As soon as $m = 2$, the energy of the chiral wave function becomes much lower than the energy of any plaquette wave function, with an energy difference of the same order of magnitude than that of the $m \rightarrow \infty$ case. Moreover, this difference increases for larger values of m . The results for $m > 1$ can be fitted linearly in $1/m$, and the slope of the fit of the chiral wave function energy is bigger than that of the plaquette wave function. Let us note that the extrapolations of the fits to the limit $m = \infty$ of the three lowest states (chiral, $0\pi\pi$ and 000 plaquettes) agree with the mean-field energies²⁹, a good test of the validity of our VMC simulations.

III. CONCLUSION

We have shown in the context of the $SU(N)$ model on the honeycomb lattice with $N = 6m$, where m is the

number of particles per site, that the presence of chiral order in the mean-field limit ($m \rightarrow \infty$) is representative of finite values of m down to $m = 2$. From that point of view, the case $m = 1$ with its plaquette ground state appears as an exception. This is an interesting step forward towards the stabilisation of chiral order in a simple Heisenberg model with only nearest neighbour permutation and no ring-exchange term. The first candidate in order of increasing N is $SU(12)$ $m = 2$. It is still too large to be realized with alkaline rare earths, which are limited to $N \leq 10$, but very close. This result suggests that a systematic investigation of $SU(N)$ models with $N \leq 10$ for all compatible values of m (i.e. values of m that divide N) and different lattice geometries might indeed reveal a case of chiral order that could be stabilized with alkaline rare earths and only nearest-neighbor permutations. Work is in progress along these lines.

We acknowledge M. Lajko and P. Nataf for useful discussions, and K. Penc for a critical reading of the manuscript. This work has been supported by the Swiss National Science Foundation.

-
- ¹ S. Sugawa, K. Inaba, S. Taie, R. Yamazaki, M. Yamashita, and Y. Takahashi, *Nature Physics* **7**, 642 (2011).
 - ² S. Taie, R. Yamazaki, S. Sugawa, and Y. Takahashi, *Nature Physics* **8**, 825 (2012).
 - ³ G. Pagano, M. Mancini, G. Cappellini, P. Lombardi, F. Schäfer, H. Hu, X.-j. Liu, J. Catani, C. Sias, M. Inguscio, and L. Fallani, *Nature Physics* **10**, 198 (2014).
 - ⁴ M. A. Cazalilla and A. M. Rey, *Reports on Progress in Physics* **77**, 124401 (2014).
 - ⁵ X. Zhang, M. Bishof, S. L. Bromley, C. V. Kraus, M. S. Safronova, P. Zoller, A. M. Rey, and J. Ye, *Science* **1467**, 1 (2014).
 - ⁶ F. Scazza, C. Hofrichter, M. Höfer, P. C. De Groot, I. Bloch, and S. Fölling, *Nature Physics* **10**, 779 (2014).
 - ⁷ C. Hofrichter, L. Riegger, F. Scazza, M. Höfer, D. R. Fernandes, I. Bloch, and S. Fölling, *Physical Review X* **6**, 021030 (2016).
 - ⁸ C. Wu, J.-p. Hu, and S.-c. Zhang, *Physical Review Letters* **91**, 186402 (2003).
 - ⁹ C. Honerkamp and W. Hofstetter, *Physical Review Letters* **92**, 170403 (2004).
 - ¹⁰ M. A. Cazalilla, A. F. Ho, and M. Ueda, *New Journal of Physics* **11**, 103033 (2009).
 - ¹¹ A. V. Gorshkov, M. Hermele, V. Gurarie, C. Xu, P. S. Julienne, J. Ye, P. Zoller, E. Demler, M. D. Lukin, and A. M. Rey, *Nature Physics* **6**, 289 (2010).
 - ¹² I. Affleck and J. B. Marston, *Physical Review B* **37**, 3774 (1988).
 - ¹³ F. F. Assaad, *Physical Review B* **71**, 075103 (2005).
 - ¹⁴ C. Xu, *Physical Review B* **81**, 144431 (2010).
 - ¹⁵ P. Corboz, M. Lajkó, A. M. Läuchli, K. Penc, and F. Mila, *Physical Review X* **2**, 041013 (2012).
 - ¹⁶ Z. Cai, H.-H. Hung, L. Wang, and C. Wu, *Physical Review B* **88**, 125108 (2013).
 - ¹⁷ T. A. Tóth, A. M. Läuchli, F. Mila, and K. Penc, *Physical Review Letters* **105**, 265301 (2010).
 - ¹⁸ P. Corboz, A. M. Läuchli, K. Penc, M. Troyer, and F. Mila, *Physical Review Letters* **107**, 215301 (2011).
 - ¹⁹ B. Bauer, P. Corboz, A. M. Läuchli, L. Messio, K. Penc, M. Troyer, and F. Mila, *Physical Review B* **85**, 125116 (2012).
 - ²⁰ P. Corboz, A. M. Läuchli, K. Totsuka, and H. Tsunetsugu, *Physical Review B* **76**, 220404 (2007).
 - ²¹ D. P. Arovas, *Physical Review B* **77**, 104404 (2008).
 - ²² M. Hermele, V. Gurarie, and A. M. Rey, *Physical Review Letters* **103**, 135301 (2009).
 - ²³ M. Hermele and V. Gurarie, *Physical Review B* **84**, 174441 (2011).
 - ²⁴ P. Corboz, K. Penc, F. Mila, and A. M. Läuchli, *Physical Review B* **86**, 041106 (2012).
 - ²⁵ H. Song and M. Hermele, *Physical Review B* **87**, 144423 (2013).
 - ²⁶ P. Corboz, M. Lajkó, K. Penc, F. Mila, and A. M. Läuchli, *Physical Review B* **87**, 195113 (2013).
 - ²⁷ J. Dufour, P. Nataf, and F. Mila, *Physical Review B* **91**, 174427 (2015).
 - ²⁸ X. G. Wen, F. Wilczek, and A. Zee, *Physical Review B* **39**, 11413 (1989).
 - ²⁹ G. Szirmai, E. Szirmai, A. Zamora, and M. Lewenstein, *Physical Review A* **84**, 011611 (2011).
 - ³⁰ S. Bieri, M. Serbyn, T. Senthil, and P. A. Lee, *Physical Review B* **86**, 224409 (2012).
 - ³¹ P. Sinkovicz, A. Zamora, E. Szirmai, M. Lewenstein, and G. Szirmai, *Physical Review A* **88**, 043619 (2013).
 - ³² P. Nataf, M. Lajkó, P. Corboz, A. M. Läuchli, K. Penc, and F. Mila, *Physical Review B* **93**, 201113 (2016).
 - ³³ H. Yokoyama and H. Shiba, *Journal of the Physical Society of Japan* **56**, 1490 (1987).
 - ³⁴ C. Gros, *Annals of Physics* **189**, 53 (1989).
 - ³⁵ A. Paramekanti and J. B. Marston, *Journal of Physics: Condensed Matter* **19**, 125215 (2007).